



# UNIANDES HEP LABORATORY

Carlos Avila

Physics Department  
Universidad de Los Andes, Colombia



- Bi-anual Particle Physics schools
- Bi-anual particle detector school
- Bi-anual Nuclear Physics school

Nuclear physics processes

Investigate  
exotic signal  
scenarios

Investigate  
BSM scenarios

4. THEORY

3. PARTICLE PHYSICS  
PHENOMENOLOGY

5. OUTREACH

UNIANDES HEP GROUP  
ACTIVITIES

1. EXPERIMENTAL  
PARTICLE PHYSICS

2. TECHNOLOGY  
TRANSFER IN RADIATION  
DETECTORS

CMS  
EXPERIMENT  
AT CERN

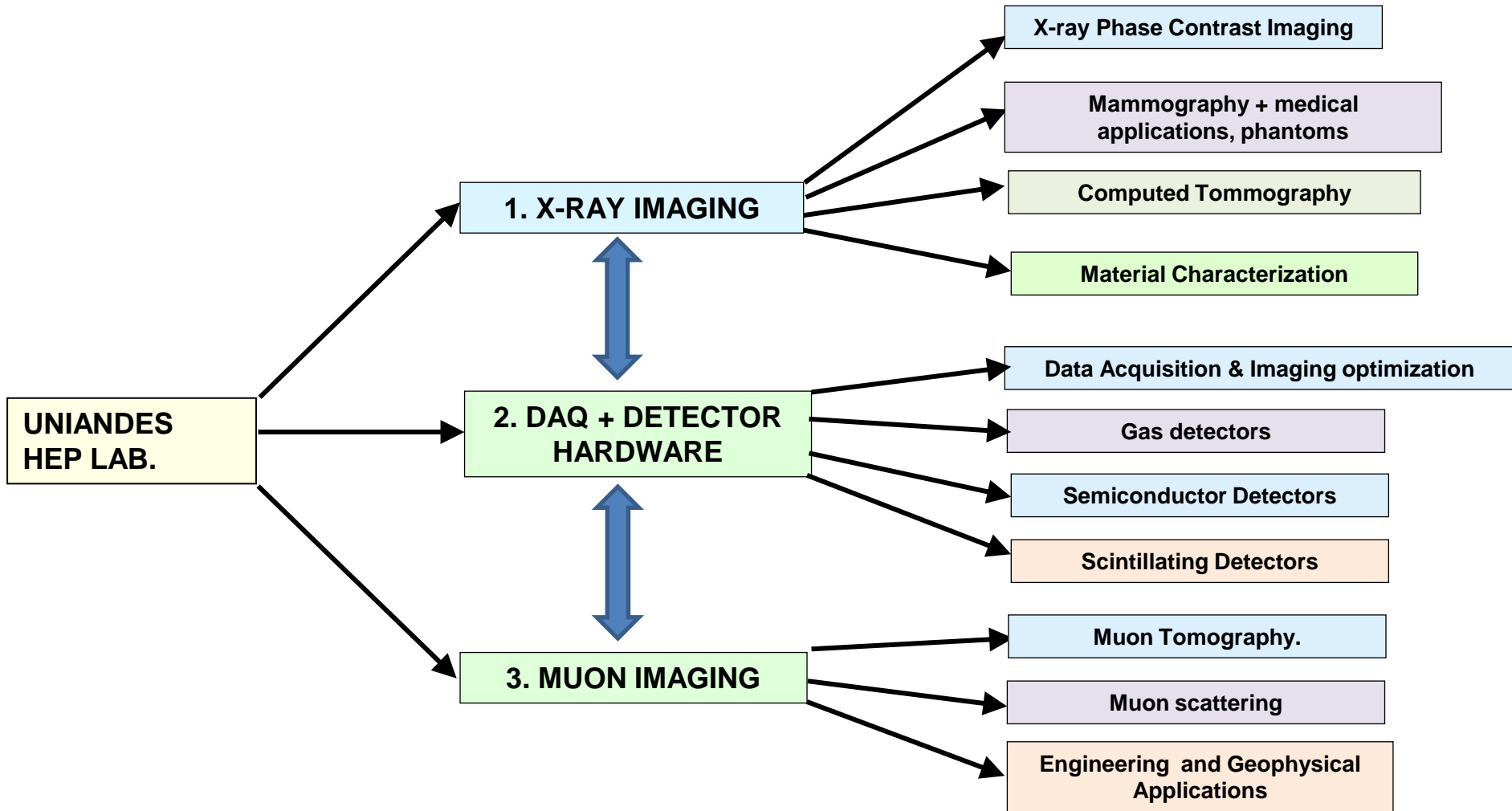
BSM  
Experimental  
searches

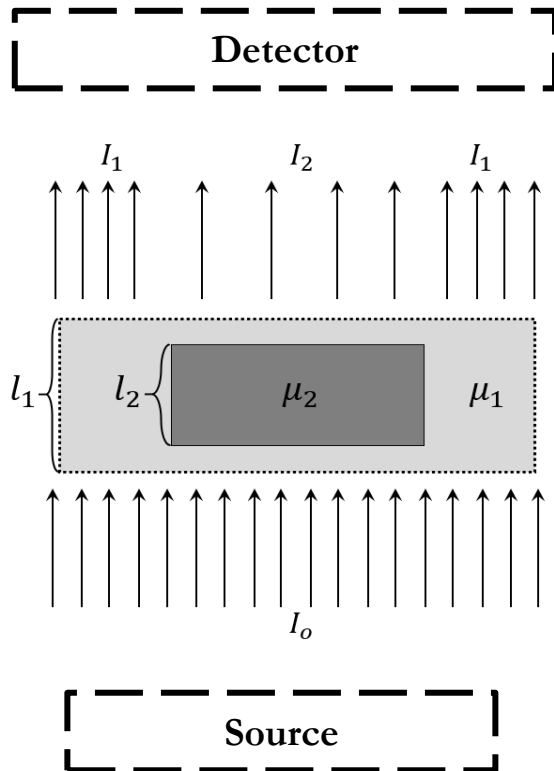
GRID  
computing  
operations

RPC muon  
detectors

X RAY IMAGING

DETECTOR HARDWARE &  
DAQ DEVELOPMENT





Starting from Beer-Lambert law:

$$I(E, z) = I_0 \text{Exp}[-\mu(E, z)z]$$

For an object embedded in a medium:

$$I_2 = I_1 \text{Exp}[-\mu_1(l_1 - l_2)] \cdot \text{Exp}[-\mu_2 l_2]$$

Contrast can be defined as:

$$C = \frac{I_1 - I_2}{I_1} = 1 - \text{Exp}(-l_2(|\Delta\mu|))$$

For polychromatic sources:

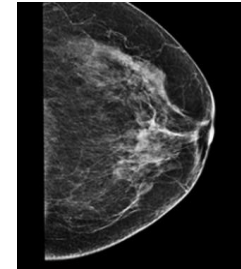
$$I(x, y) = \int I_0(x, y) e^{-(\mu_1^\lambda - \mu_2^\lambda)T_0(x, y)} D(\lambda) d\lambda$$



# X ray phase contrast imaging

Many biological and human tissues are soft: they have low X-ray absorption → they are difficult to visualize with conventional X ray techniques:

- 2 specific cases:
- Breast Tissue
  - Blood Vessels (without a contrast agent)



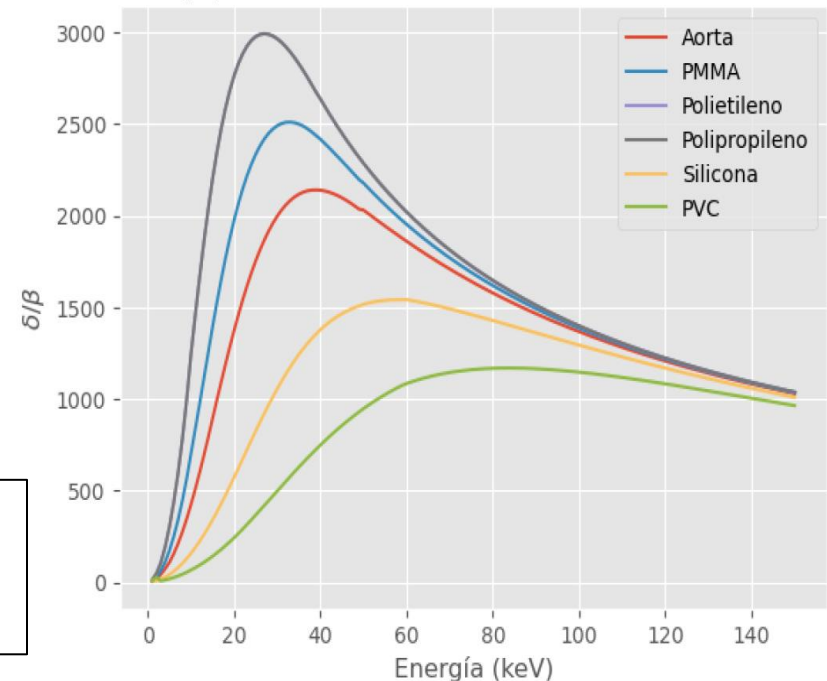
The EM wave propagating through the sample is  $\psi = \psi_0 \exp\left(i \frac{n\omega}{c} z\right)$

In the x ray energy range the index of refraction can be written as :  $n = 1 - \delta + i\beta$



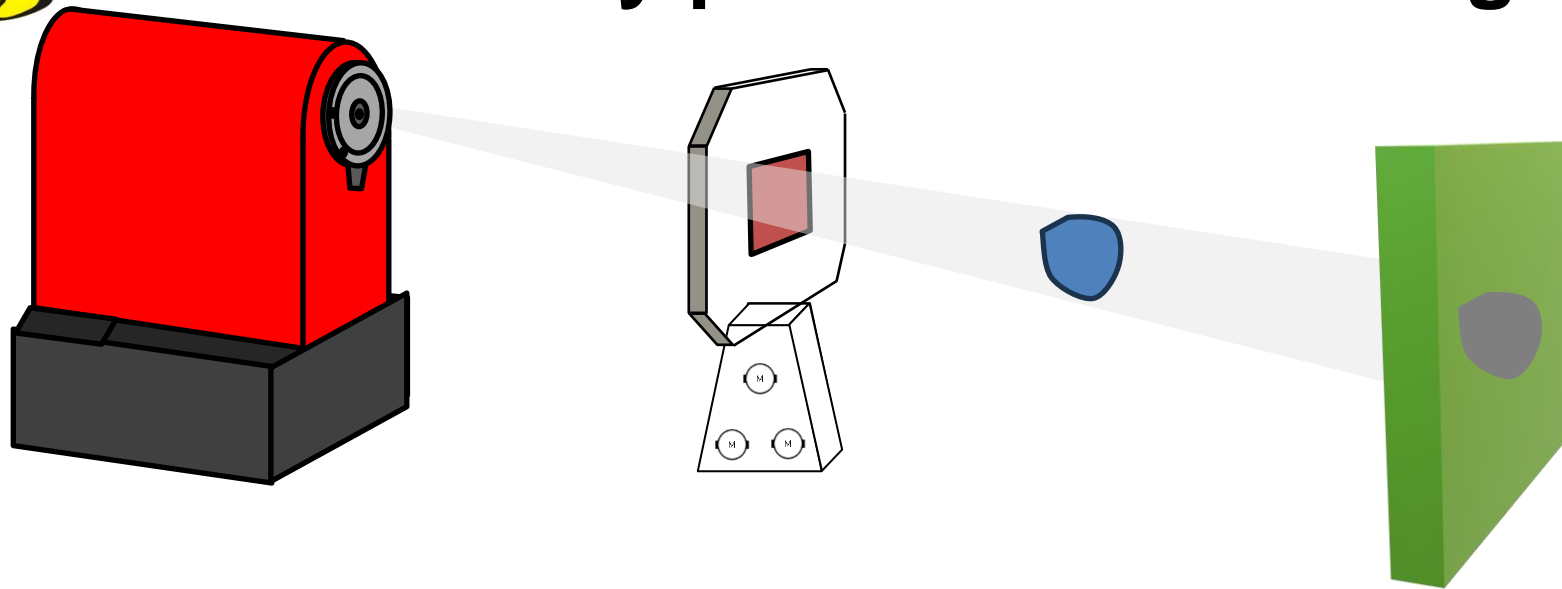
- Phase effects are produced by  $\delta$
- Attenuation effects are caused by  $\beta$

For many soft tissues  $\delta$  is ~ 3 orders of magnitude greater than  $\beta$  → phase effects could enhance Image contrast





# X ray phase contrast imaging



- A microfocus X –ray source is required (focal spot of  $\sim \mu\text{m}$ ) to have a high spatial coherent beam
- A high resolution detector is needed to observe small changes in intensity due to phase variations
- Photon energy measurements by the detector will allow to perform spectral image análisis.
- A grating ( a mask or sand paper) diffracts the X-ray beam producing a known phase shift, allowing to measure the phase shift induced by the sample.
- Specialized phase-retrieval algorithms need to be applied to the final image.

# UNIANDES X RAY TEST SETUP

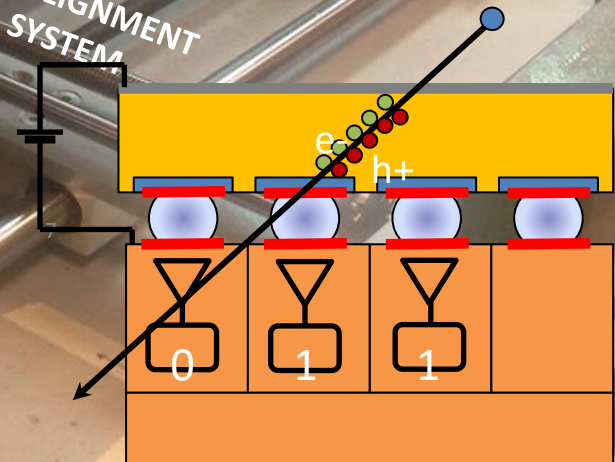
## X-ray Source Technical Specs

- Hamamatsu L10321
- W Anode,  $\mu$ Focus ( $5\mu\text{m}$ )
- Voltage:  $0\text{kVp}$  to  $100\text{kVp}$
- Current:  $0\mu\text{A}$  to  $200\mu\text{A}$
- Continuous Emission
- Air Cooling

MICROFOCUS  
X RAY TUBE

TIMEPIX  
DETECTOR

ALIGNMENT  
SYSTEM



# UNIANDES X RAY TESTING SETUP



## X-ray Shielding Cabinet

Steel casing over Pb shielding  
 Pb glass  
 Heat Exhaust port  
 Dimensions: 2m x 1m x 0.8m

## Safety Interlocks

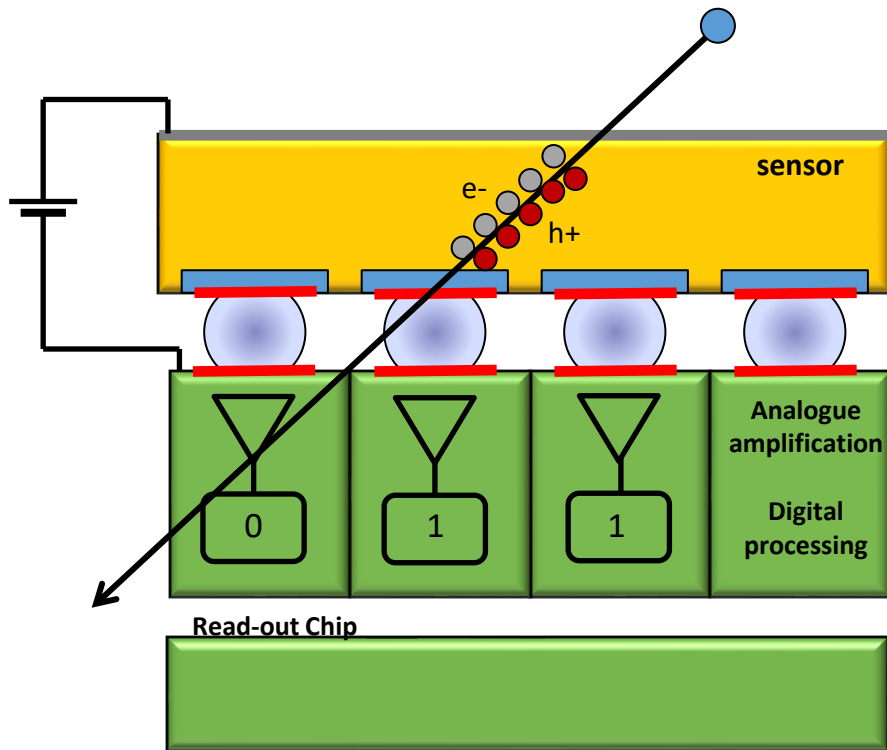
→ Temperature (24°C max)  
 → Door  
 → Software Comm (3s poll time)  
 → External Timer

## Positioning System w/ 4 axis

X: 10 $\mu$ m/step  
 Y: 1.25 $\mu$ m/step, with position sensor  
 Z: 10  $\mu$ m/step  
 $\theta$ : 0.03°/step



# MEDIPIX Detector



An incident photon generates e-hole pairs

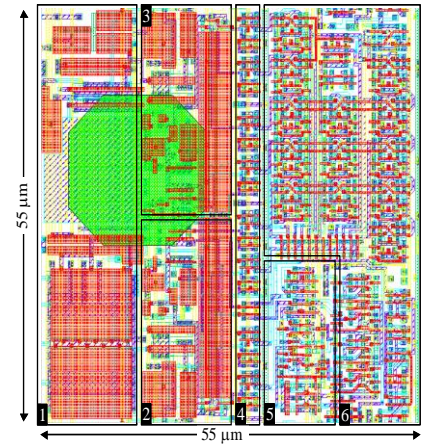
The reverse biasing of the sensor diode structure drives the charge to the readout chip

The charge is shaped and a threshold applied

Digital processing and readout occurs

The data is read out off the chip

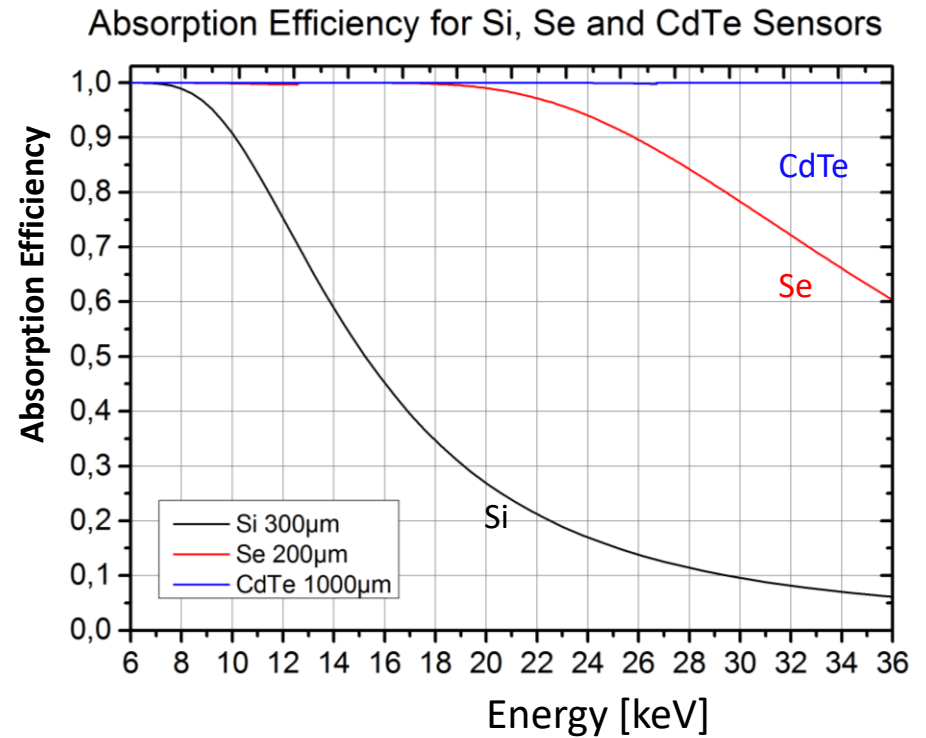
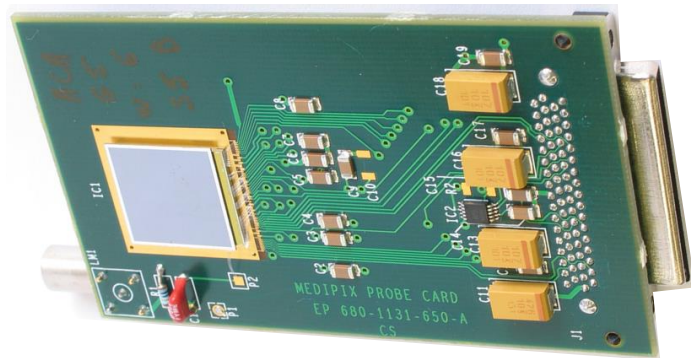
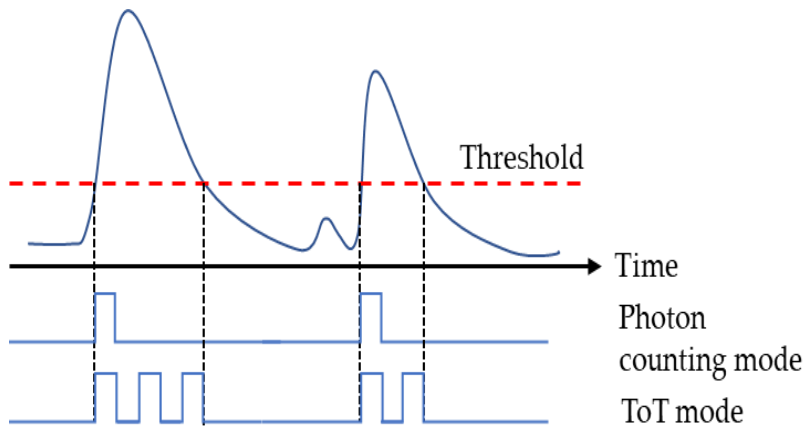
## Electronics for 1 pixel:



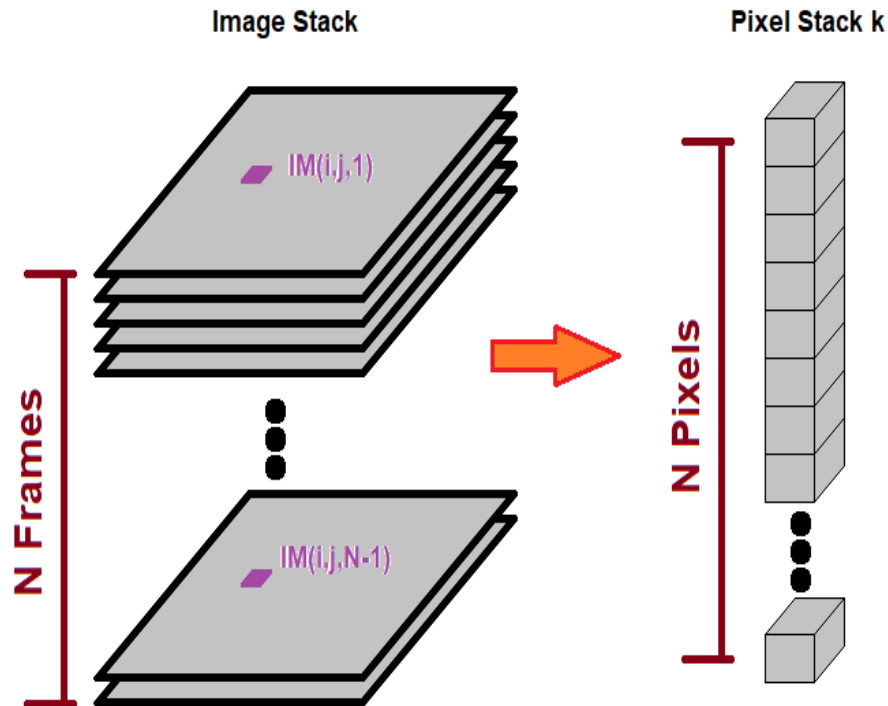
- **Analog side:**  
Preamplifier, High Level Discriminator, Low Level Discriminator, 8-bit Pixel memory
- **Digital side:**  
Window discrimination logic, 13-bit Counter  
**>500 transistors/pixel**

# SPECIAL FEATURES OF THE TIMEPIX3 DETECTOR

Timepix3 detector working principle.



# DAQ METHODOLOGY



## Dataset:

- Frame stack with at least 6x Full dose
- 5s frames

## Dose Reconstruction:

- Sum frames equal to desired dose

## Flat Field Mask:

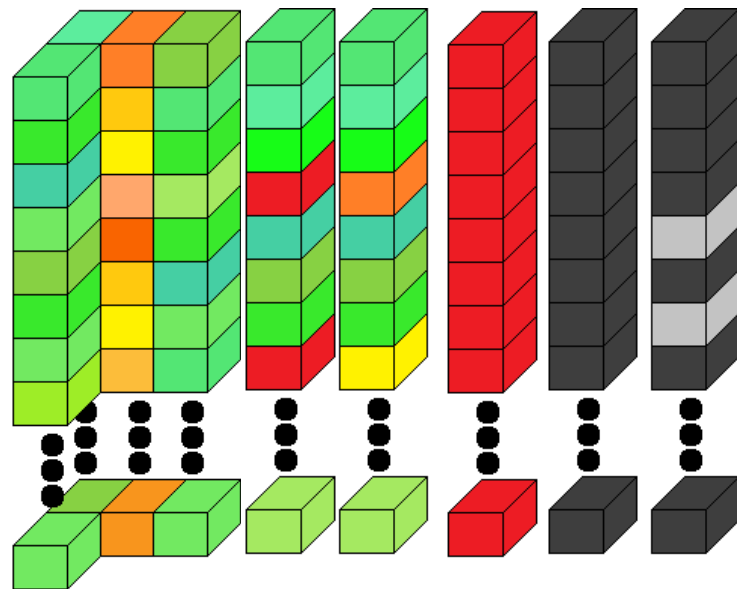
- As much dose as possible, considering detector stability in time

# NOISY PIXEL CORRECTIONS

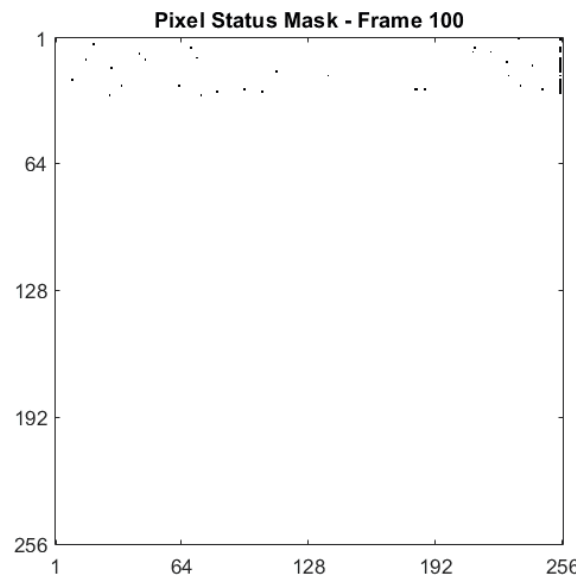
## Malfunctioning Pixel Analysis



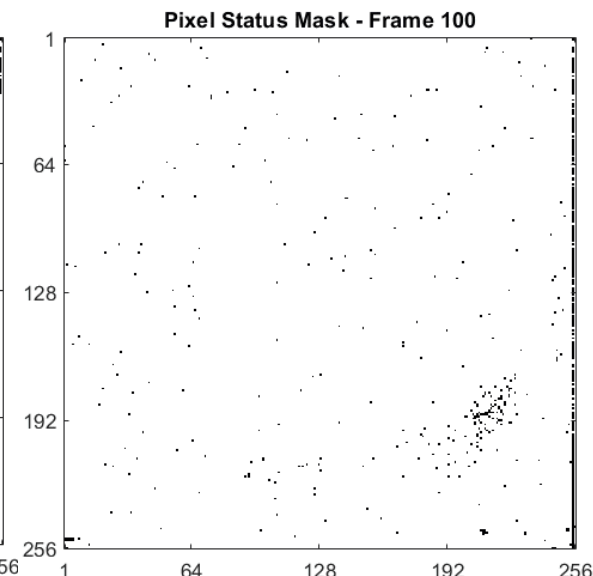
## Correction Masks 8-Neighbor Interpolation



Noisy Pixels – 1 frame



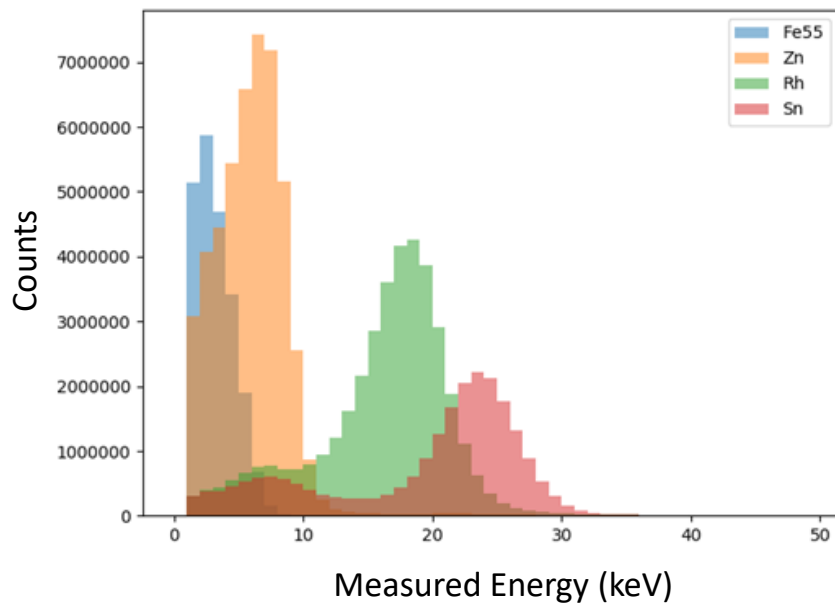
Noisy Pixels – Various frames



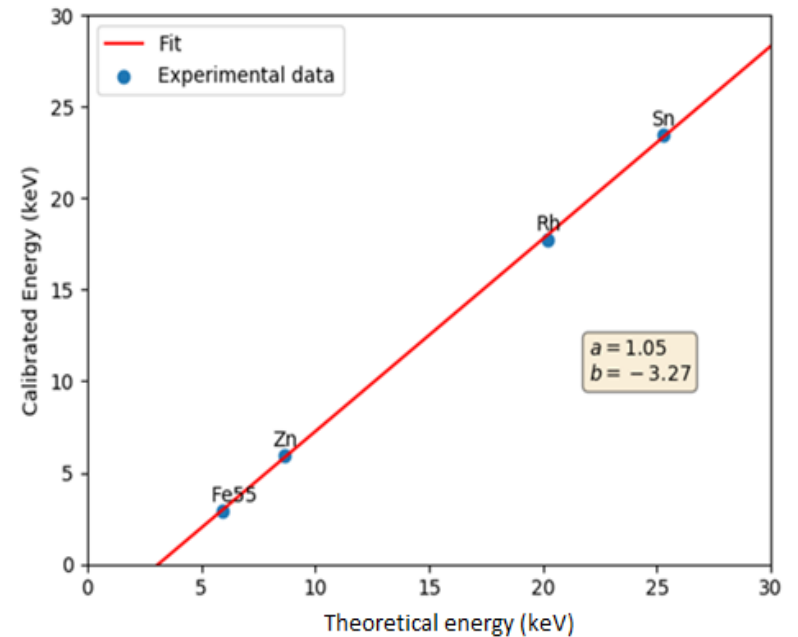
# ENERGY CALIBRATION

- Linearity of the calibration with X-ray fluorescence and Radioactive Fe-55

Histograms of the X-ray fluorescence and Radioactive (Fe-55) spectrums

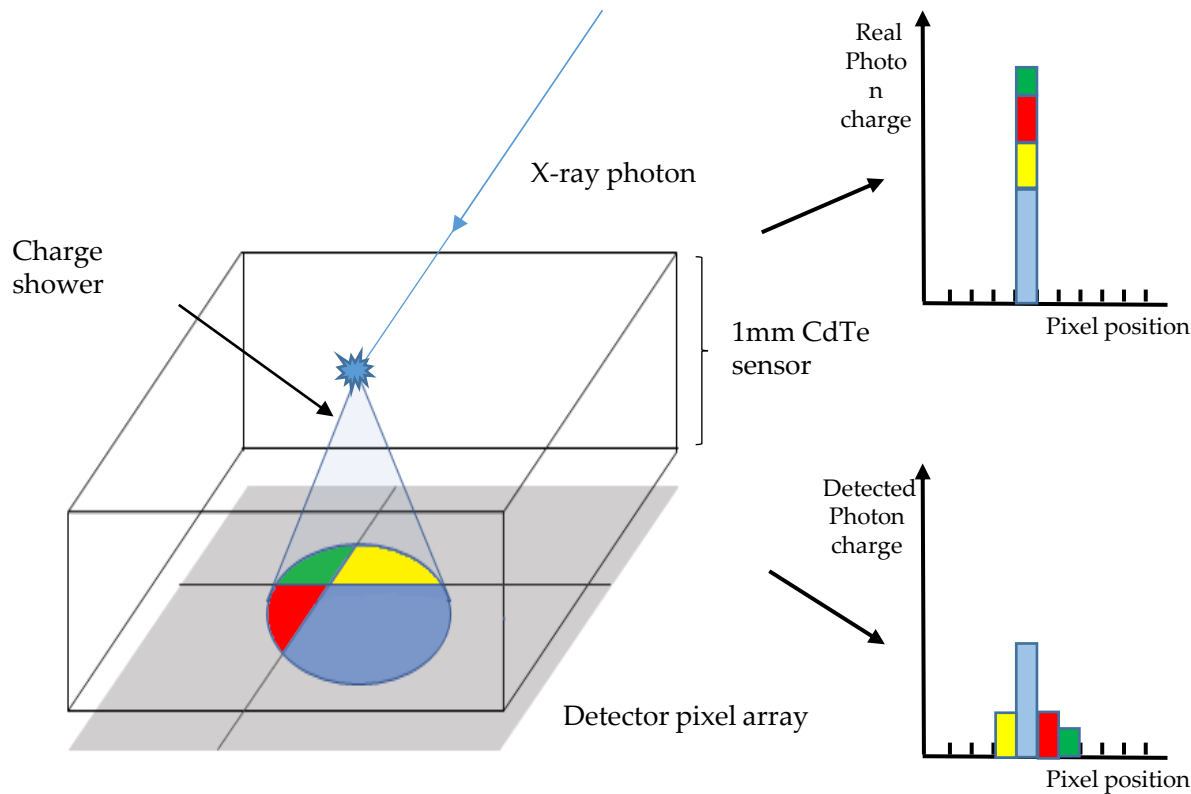


Energy calibration linearity of the Timepix3 detector



# CHARGE SHARING + CLUSTERING

- Charge-sharing in Photon-counting detectors



Charge-sharing increases with:

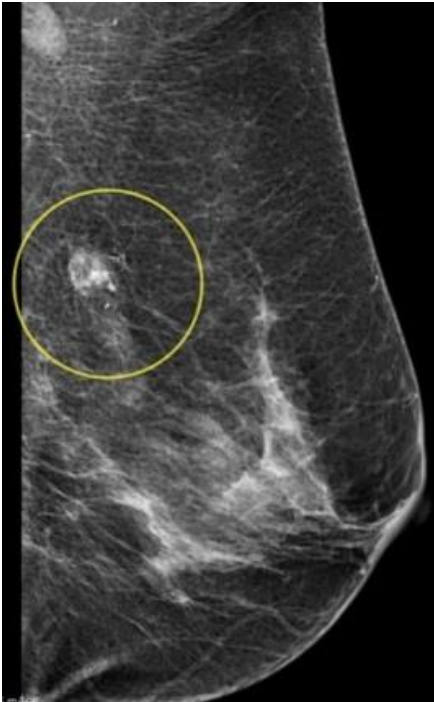
- Sensor thickness.
- Smaller pixel pitch.
- Lower bias voltage.

Three methods:

- **Unclustered** Image.
- **One-pixel clusters:** Only events that took place in a single pixel.
- **'Full clusters':** All pixel size clusters. Energy volume is allocated to the pixel closer to the cluster centroid.

**Requires individual photon energy information.**

# MAMMOGRAPHY APPLICATIONS



- Microcalcifications present in malignant breast tumors are composed mainly of Calcium Hydroxiapatyte.<sup>1</sup>

- Benefit of mammography screening could be reduced due to the risk of radiation-induced tumors.<sup>2</sup>

Early diagnosis of breast cancer is vital for increased survival, with the lowest possible radiation exposure!

<sup>1</sup> M. C. Jansen-van der Weide, M. J. Greuter, L. Jansen, J. C. Oosterwijk, R. M. Pijnappel, and G. H. de Bock, Eur Radiol, vol. 20, no. 11, pp. 2547-2556, Nov. 2010 .

# IMAGING SETUP - COMMERCIAL DEVICE

Hologic Selenia Dimensions w/ AWS5000



## X-ray Source Technical Aspects

- W anode
- 50 $\mu$ m Rh filter
- Operated at 28kVp
- High power: 7kW
- Focal Spot size > 100 $\mu$ m

## X-ray Detector Technical Aspects

- a-Se Direct Conversion FPD
- 200 $\mu$ m thickness
- 70 $\mu$ m pixel pitch
- Charge-Integration

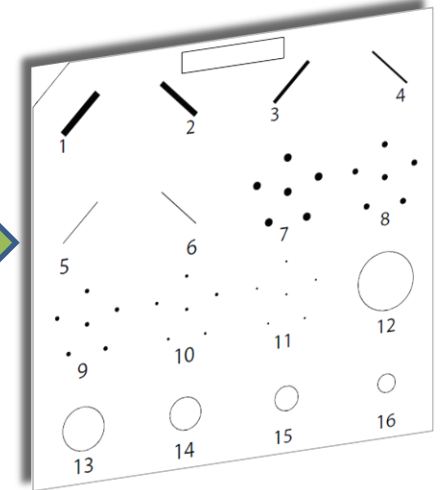
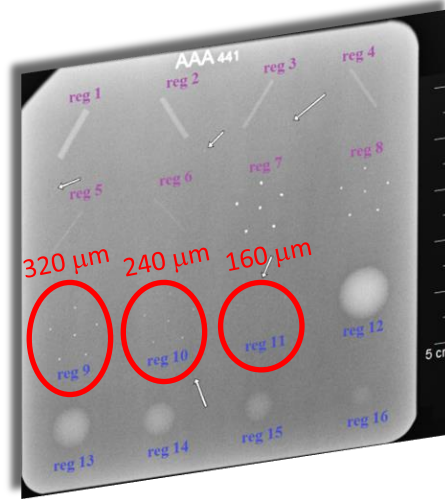
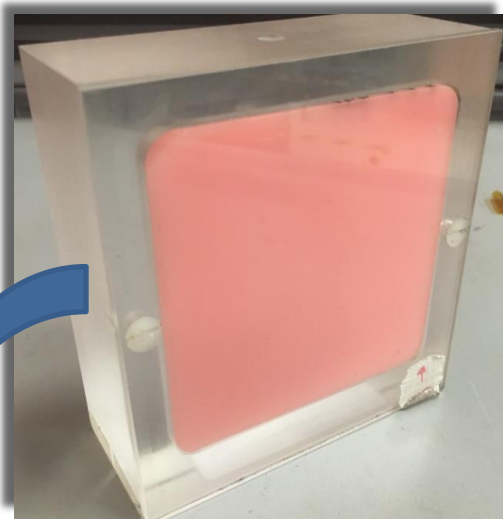
## X-ray Imaging Geometry

- Source-Detector Distance: 70cm
- Source-Object Distance: 63cm

5 Selenia Dimensions with AWS 5000 – A flexible platform for the next dimension in breast imaging, Hologic Inc., Marlborough, MA, 2011



# APPLICATIONS IN MAMMOGRAPHY

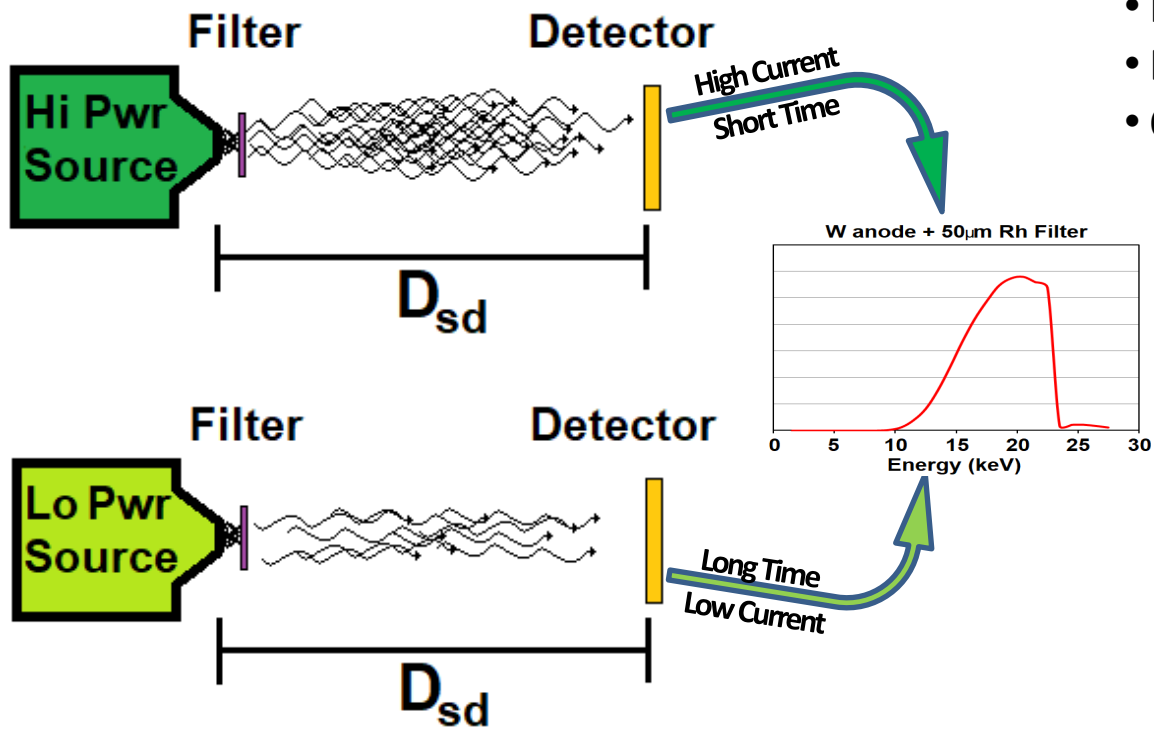


WAX INSERT					
FIBERS (Nylon Fiber)		SPECKS (Al <sub>2</sub> O <sub>3</sub> speck)		MASSSES (Thickness)	
1.	1.56 mm	7.	0.54 mm	12.	2.00 mm mass
2.	1.12 mm	8.	0.40 mm	13.	1.00 mm mass
3.	0.89 mm	9.	0.32 mm	14.	0.75 mm mass
4.	0.75 mm	10.	0.24 mm	15.	0.50 mm mass
5.	0.54 mm	11.	0.16 mm	16.	0.25 mm mass
6.	0.40 mm		-		-

**Mammography  
Accreditation  
Phantom CIRS,  
model 015**

# DOSE CALIBRATION

Both setups generate the same spectrum, with different intensities



## Timepix Si Detector as Dose Calibrator:

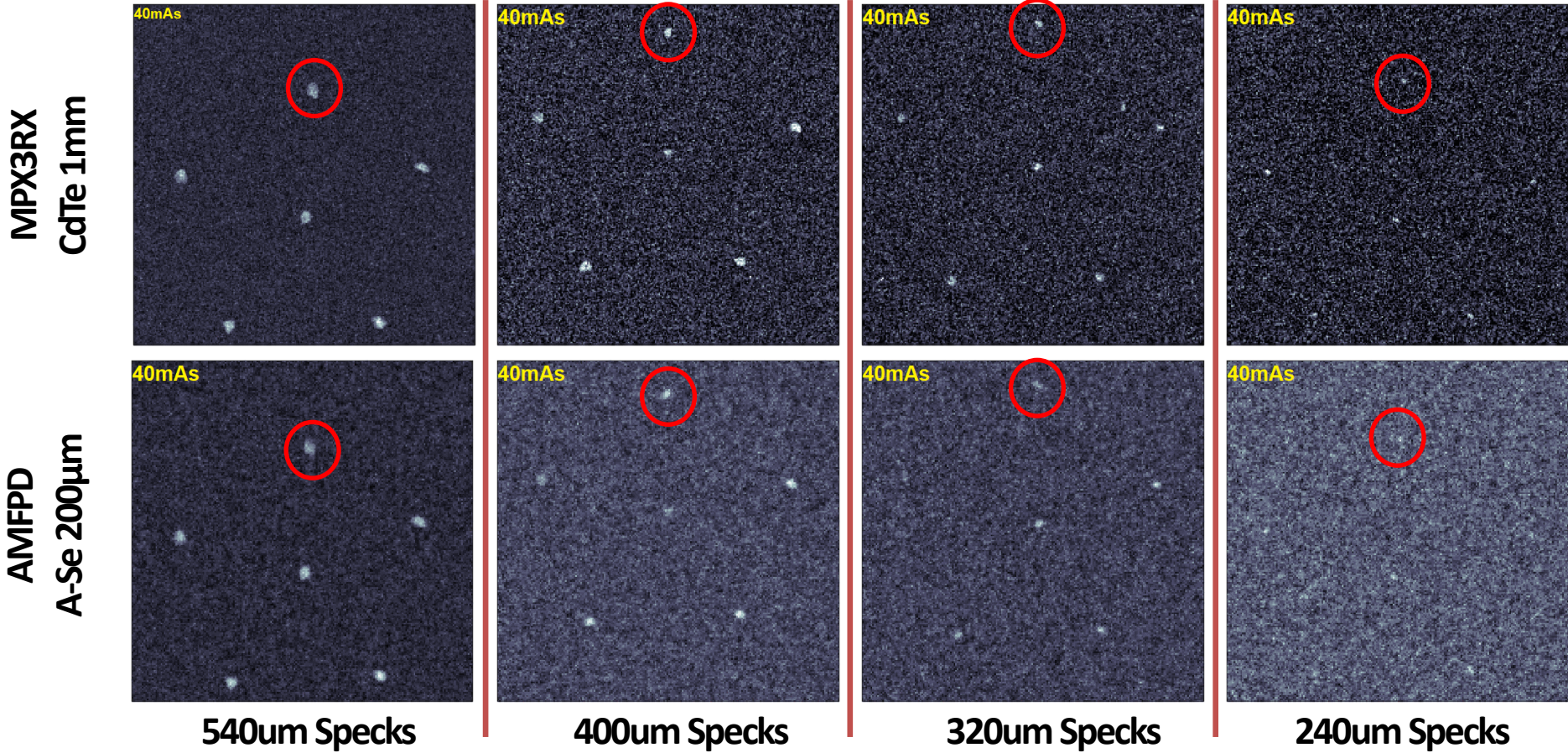
- Highly stable detector
- Fast Acquisition Times: 1 $\mu$ s – 10 $\mu$ s
- ESD [mGy]  $\rightarrow$  total photon counts
- Cts/s and source pulse characterization

### 6 Dose

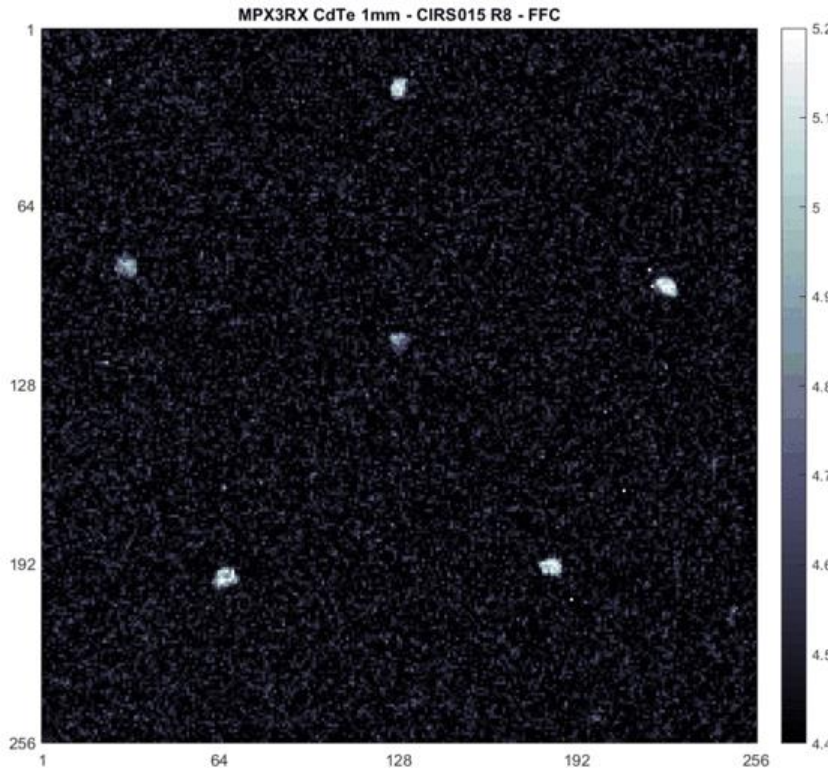
#### Measurements:

- 40mAs  $\rightarrow$  1.79 mGy
- 50mAs  $\rightarrow$  2.09 mGy
- 60mAs  $\rightarrow$  2.52 mGy
- 70mAs  $\rightarrow$  2.95 mGy
- **80mAs  $\rightarrow$  3.36 mGy**
- 90mAs  $\rightarrow$  3.79 mGy

# PHANTOM X-RAY IMAGES



# CNR - SPECK SEGMENTATION

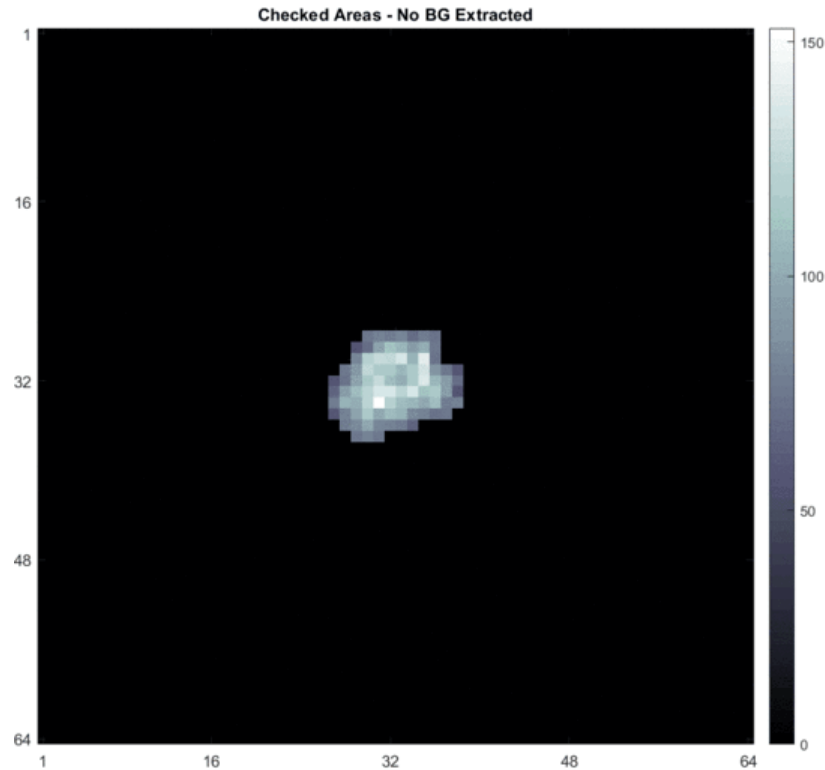


$$CNR = \frac{S - \bar{B}}{\sigma_B}$$

Signal Calculation

$$S = \sum_k s_k$$

# CNR - BACKGROUND SAMPLING



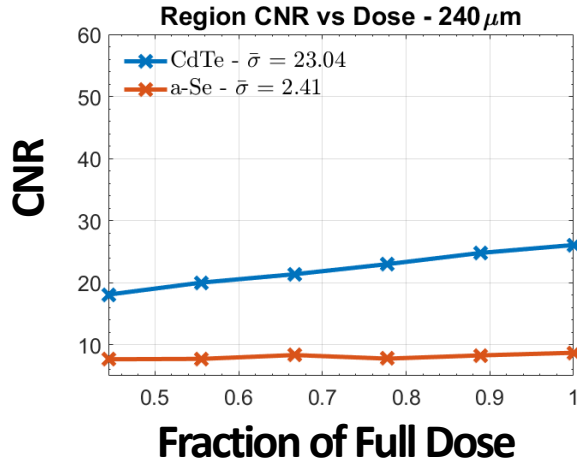
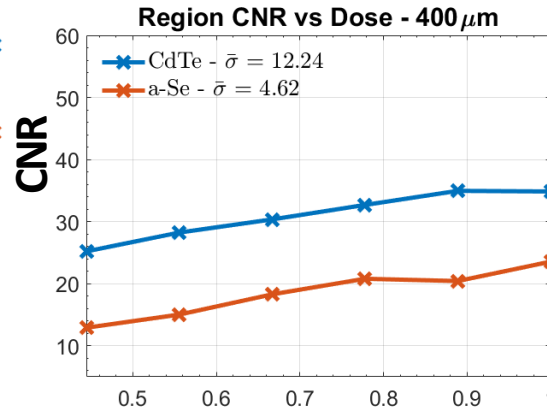
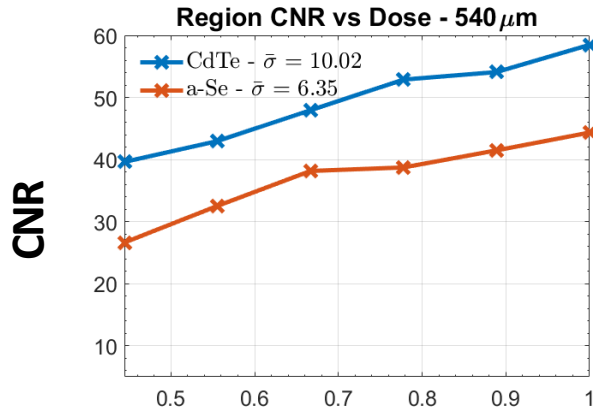
Background Calculation

$$\bar{B} = \frac{1}{N} \sum_{i=1}^N \sum_k (b_k)_i = \frac{1}{N} \sum_{i=1}^N B_i$$

Noise Calculation

$$\sigma_B = \sqrt{\frac{1}{N} \sum_{i=1}^N (\bar{B} - B_i)^2}$$

# RESULTS – CNR PER REGION



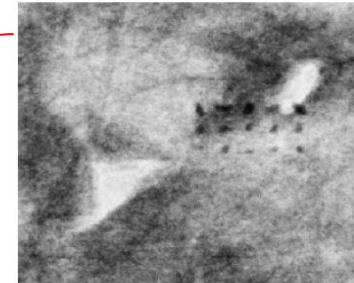
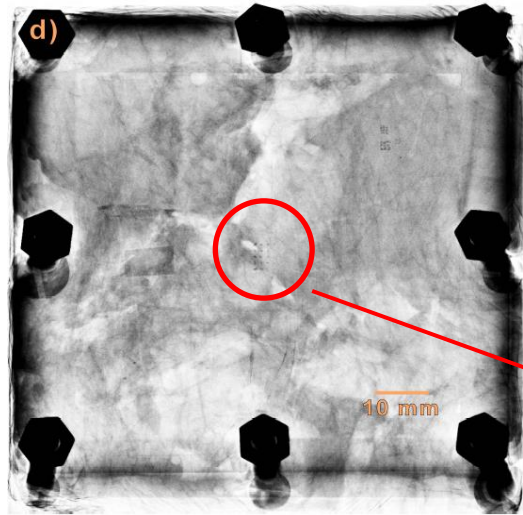
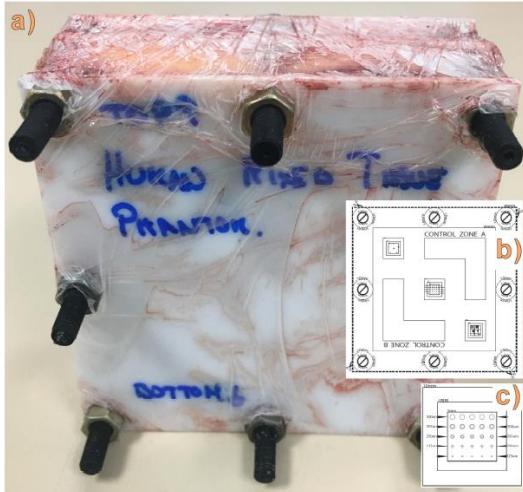
1.1X to 38X

- Average CNR for photon counting CdTe detector is greater at all doses and all speck sizes.
- Standard image quality could be achieved with lower radiation doses.
- MDPX + CdTe has better resolution for smaller crystal sizes which could be critical for early diagnosis.

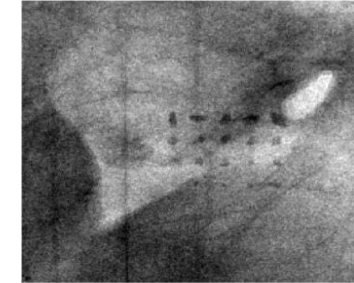
Study of Contrast-to-Noise Ratio performance of a Medipix3RX CdTe detector for low dose mammography imaging  
 Gerardo Roque <sup>a,\*</sup>, Carlos Avila <sup>a</sup>, Maria L. Pérez-Lara <sup>a</sup>, Luis Mendoza <sup>b</sup>, Simon Procz <sup>c</sup>  
<sup>a</sup> Departamento de Física - Universidad de los Andes, Cra. 1 No. 184-12, 111711, Bogotá D.C., Colombia  
<sup>b</sup> Departamento de Física - Universidad Militar Nueva Granada, 110221, Cra. 11 No. 101-80, Bogotá D.C., Colombia  
<sup>c</sup> Freiburger Materialforschungszentrum - Albert-Ludwigs-Universität Freiburg, Stefan-Meier-Straße 21, 79104 Freiburg i. Br., Germany  
 Nuclear Inst. and Methods in Physics Research, A 992 (2021) 165000


 PUBLISHED BY IOP PUBLISHING FOR SISSA MEDIALAB  
 RECEIVED: September 16, 2023  
 ACCEPTED: October 24, 2023  
 PUBLISHED: ???, 2023  
 TECHNICAL REPORT  
**CNR performance of semiconductor materials for X-ray imaging of breast calcifications**  
 L. Mendoza,<sup>a,\*</sup> C. Avila,<sup>b</sup> R. Rodriguez,<sup>b</sup> L. Loalza<sup>c</sup> and G. Roque<sup>b</sup>

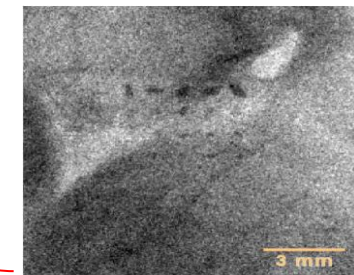
# TESTS WITH A HUMAN BREAST TISSUE PHANTOM



Hologic Selenia, Se-detector



1 mm CdTe-Medipix3RX



0.5 mm Si-Medipix3RX

Phantom constructed with breast Human tissue and with hidroxiapatite crystals embedded artificially by us. Tissue donated by a patient with breast reduction.

X-RAY image taken with a Selenia mammographic system of the Brest human phantom.

All ethical protocols and permissions were followed.

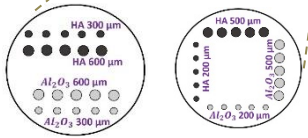
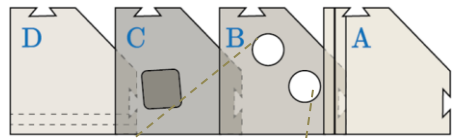
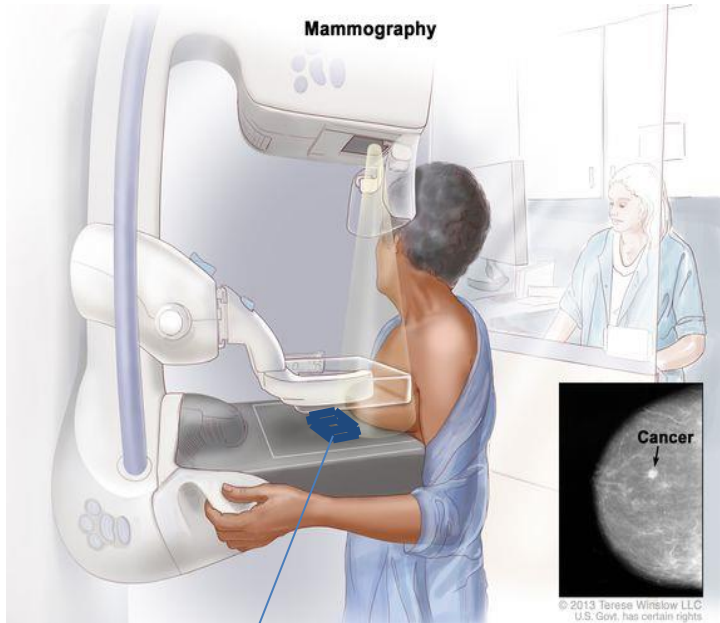
Sept. 16 2024

Investigation of CdTe, GaAs, Se and Si as Sensor Materials for Mammography

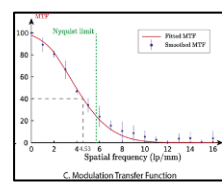
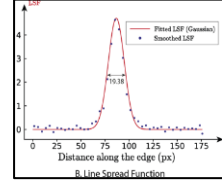
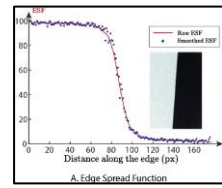
Simon Procz<sup>✉</sup>, Gerardo Roque, Carlos Avila, Jorge Racedo<sup>✉</sup>, Student Member, IEEE, Roberto Rueda, Ivan Santos, and Michael Fiederle

IEEE TRANSACTIONS ON MEDICAL IMAGING, VOL. 39, NO. 12, DECEMBER 2020

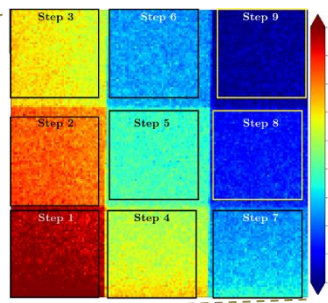
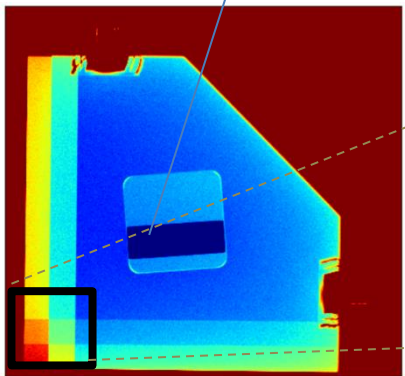
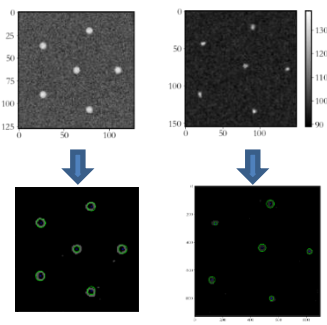
# IMPROVING PHANTOM REQUIREMENTS FOR MAMMOGRAPHY STUDIES



## Microcalcifications



Interpolation of known lesions to diagnose real lesions: Phantom Breast



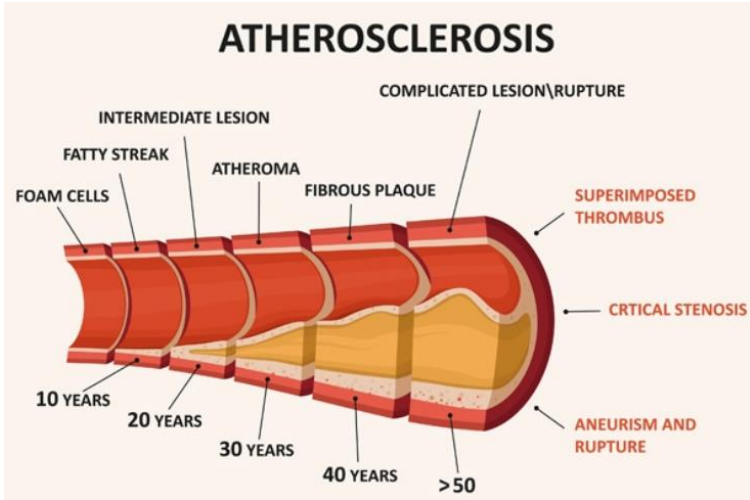
Diagnostic + calibration phantom for simultaneous Xray images with patients, allow:

- 1) MTF, CNR in-vivo calibration equipment measurements.
- 2) Diagnostic guide of microcalcification imaging vs breast composition.

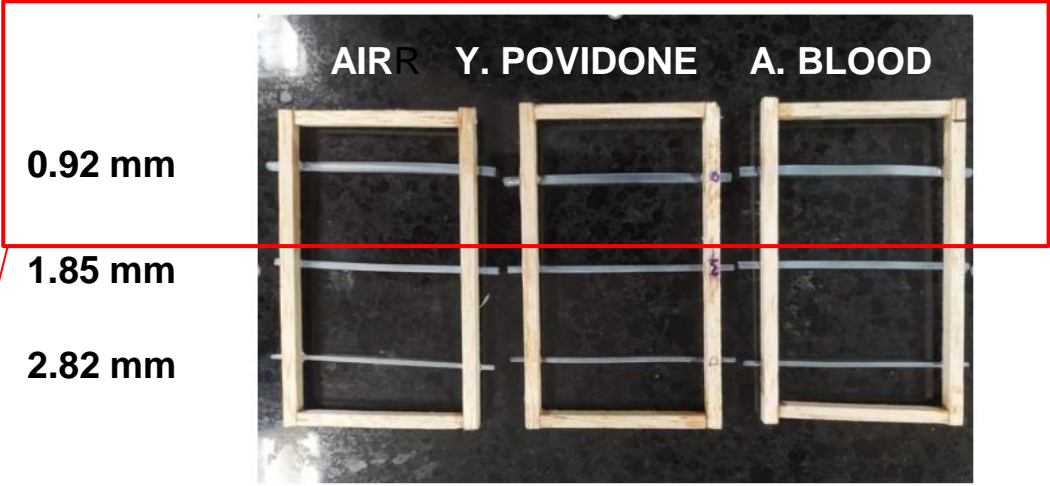
**Patent:** C. Avila. G. Roque, J. S. Calderon, Patente, “Fantoma de Calibración y diagnóstico”, Octubre 2022, SIC 054-2019



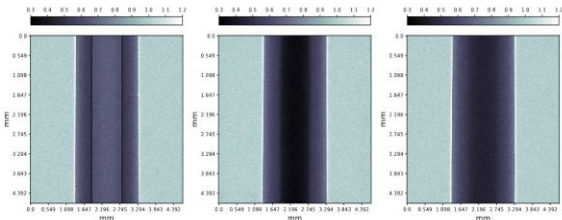
# Impact of phase retrieval in Angiography



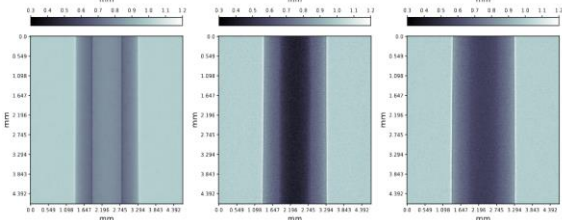
<https://www.medicoverhospitals.in/diseases/atherosclerosis/>



Raw Images



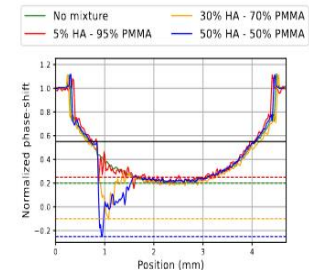
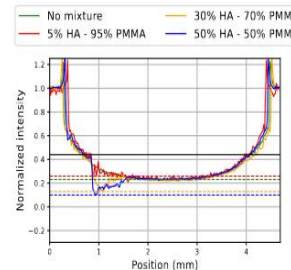
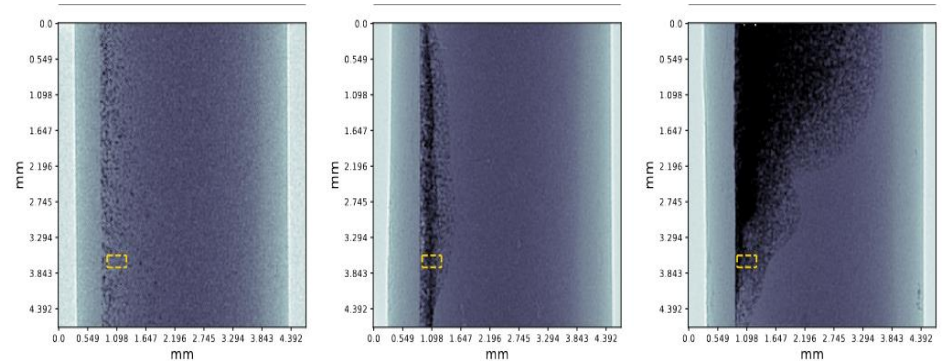
Phase Images



5% plaque

30% plaque

50% plaque



Plaque + A. blood  
No contrast agent

Phase retrieval contributes to enhance Image contrast → plaque can be observed without any contrast agent

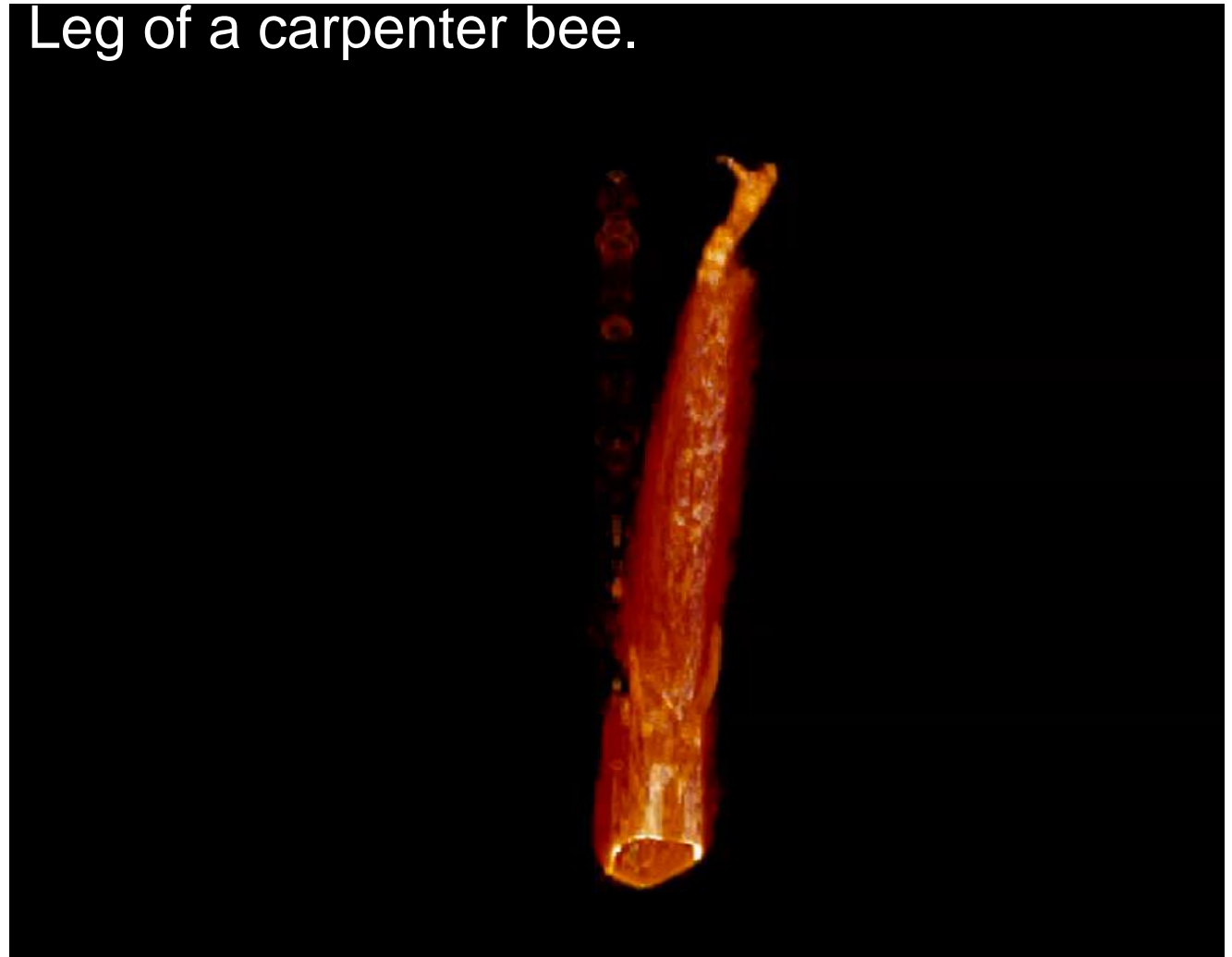
Results submitted to Phys. Med. Biol.

Raw Images

Phase Images

# MICRO COMPUTED TOMOGRAPHY

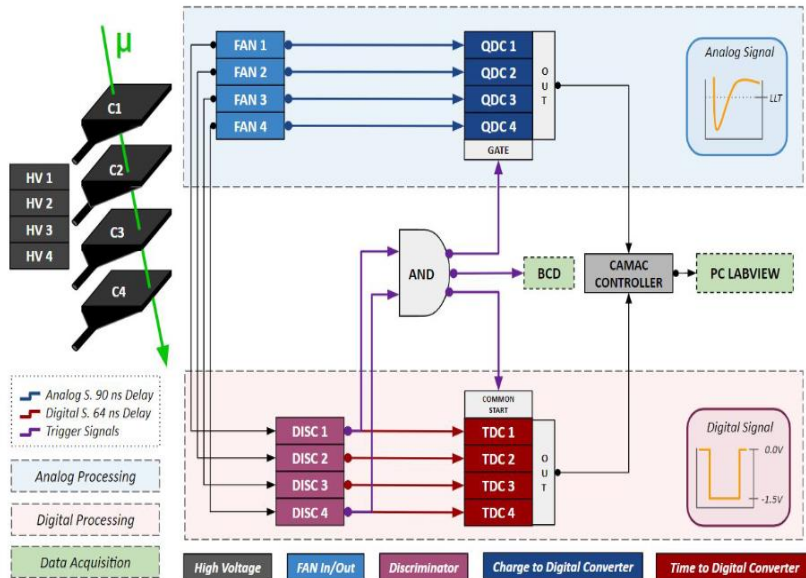
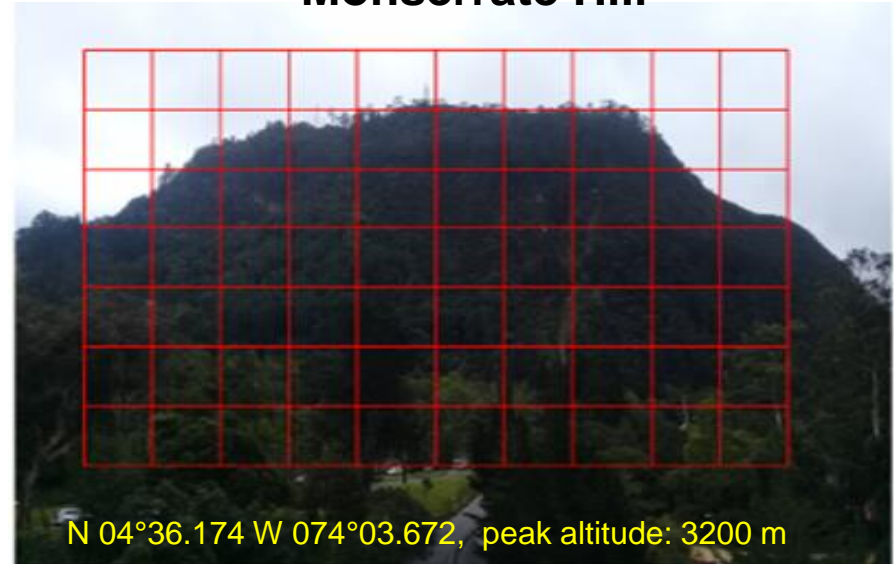
## Leg of a carpenter bee.



- A X20 magnification factor can be achieved to increase pixel resolution to about 3  $\mu\text{m}$ .
- our setup can take up to 3600 different projections for high resolution 3D images.
- We are working on configuring PCI and spectral CT's

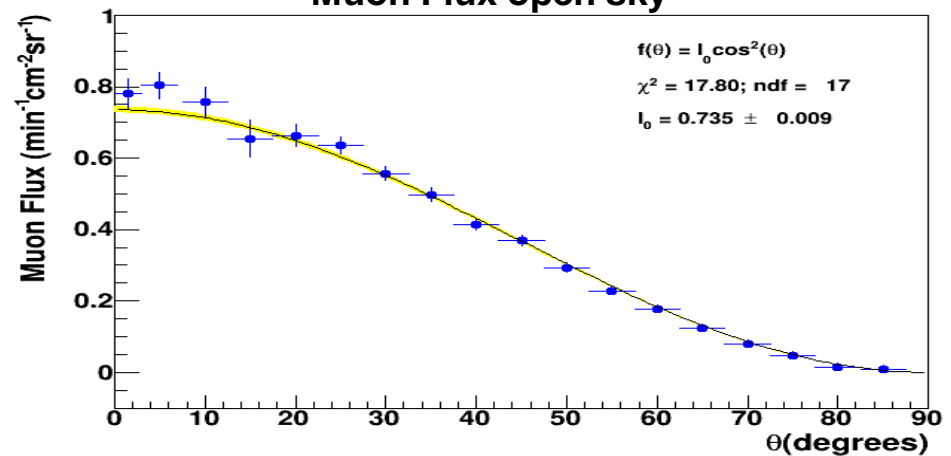


## Montserrat Hill



**Muon flux at Bogotá =  $1.53 \pm 0.03 \text{ cm}^{-2} \text{ s}^{-1}$**

## Muon Flux open sky

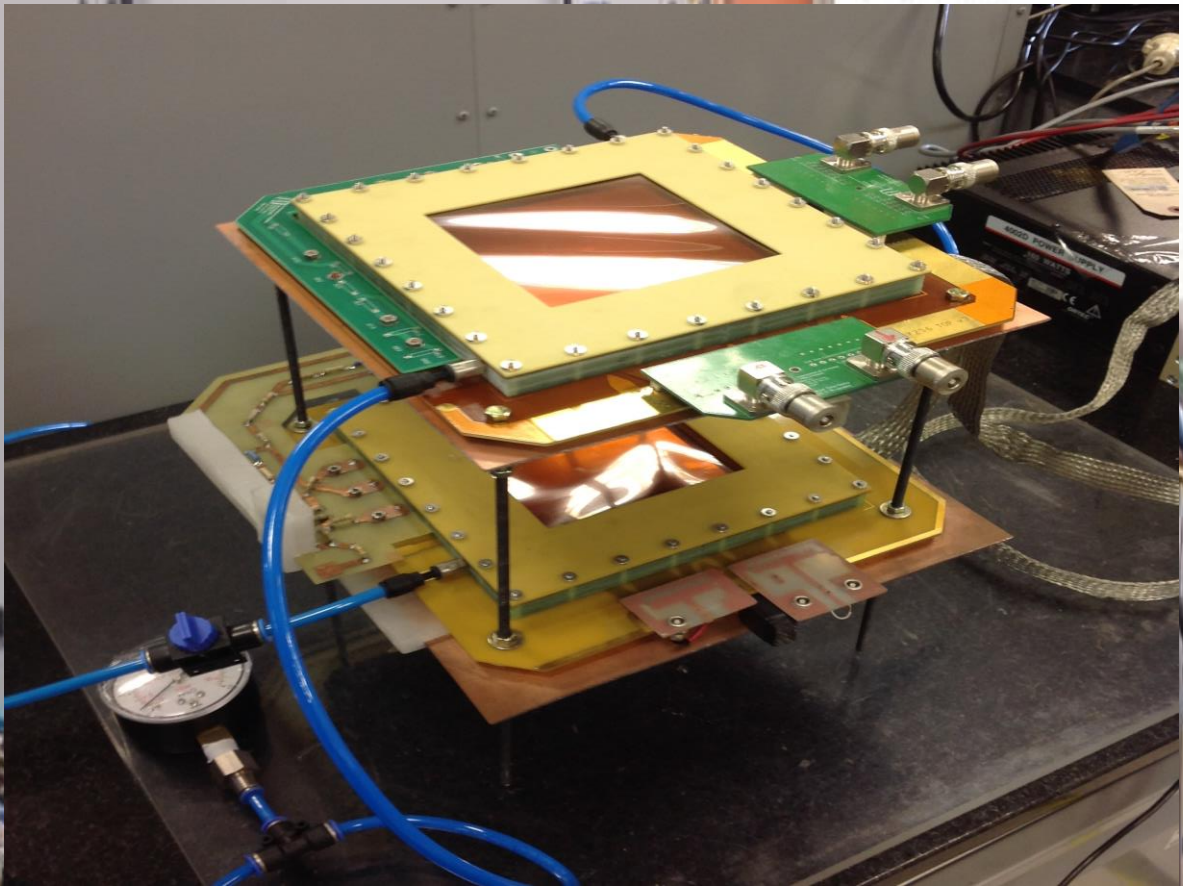
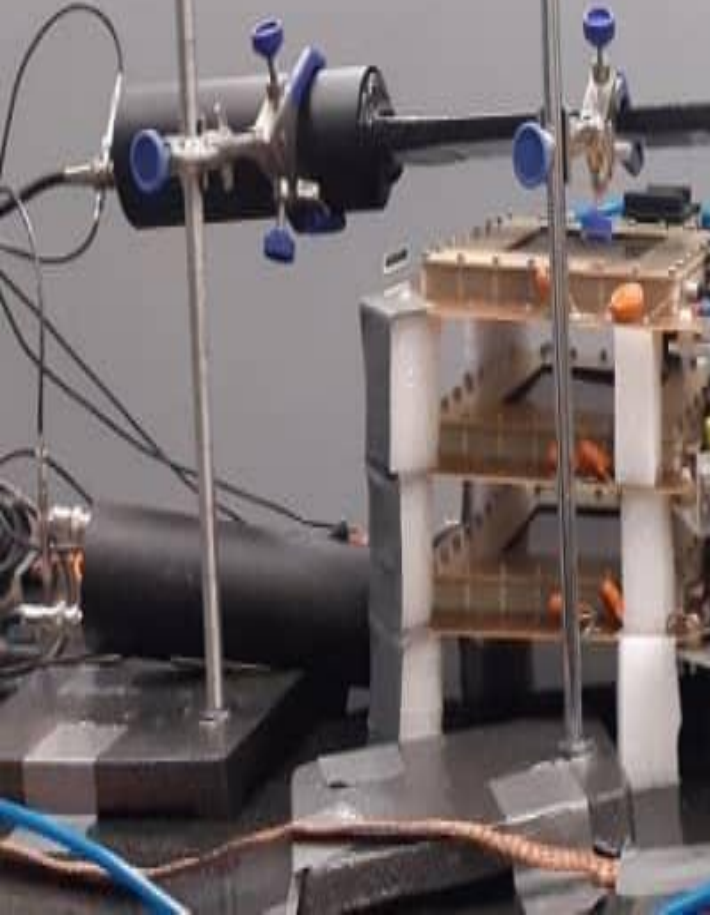


**instruments** **MDPI**

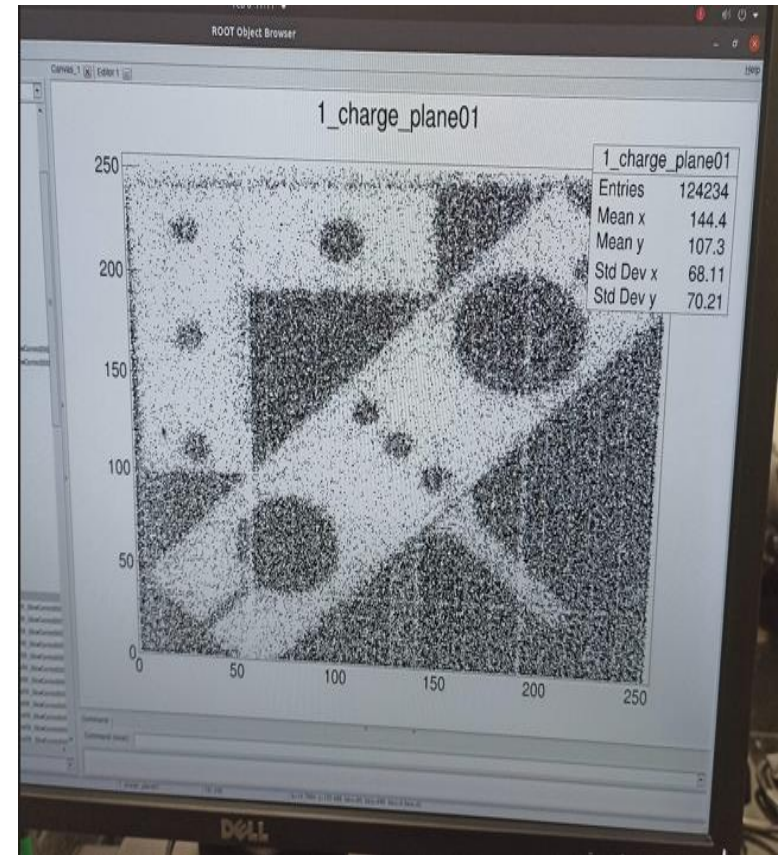
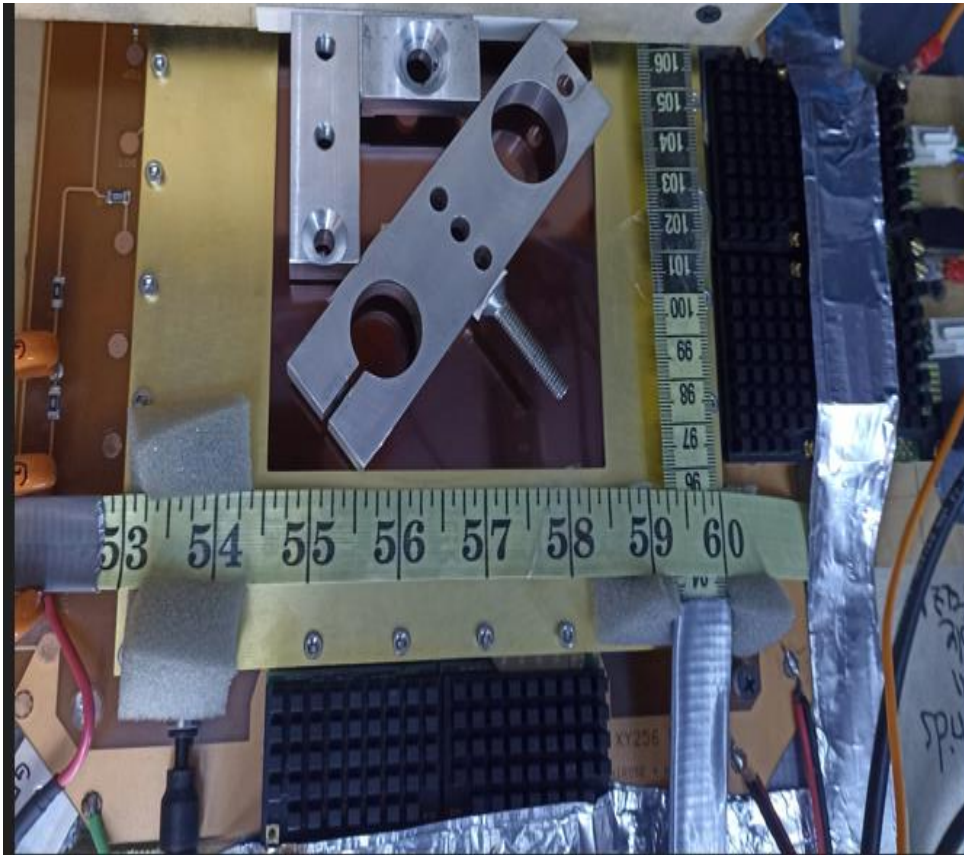
Article  
**Atmospheric Muon Flux Measurement near Earth's Equatorial Line**  
 Cristian Borja <sup>\*,†</sup>, Carlos Ávila <sup>†</sup>, Gerardo Roque <sup>✉</sup> and Manuel Sánchez <sup>\*</sup>

Instruments 2022, 6(4), 78; <https://doi.org/10.3390/instruments6040078>

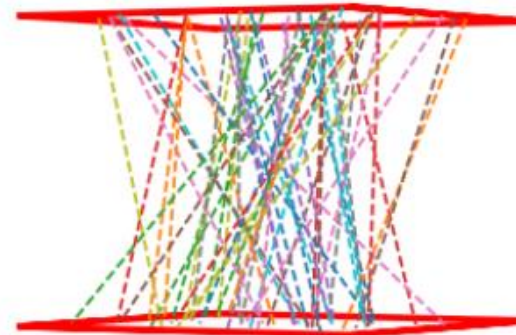
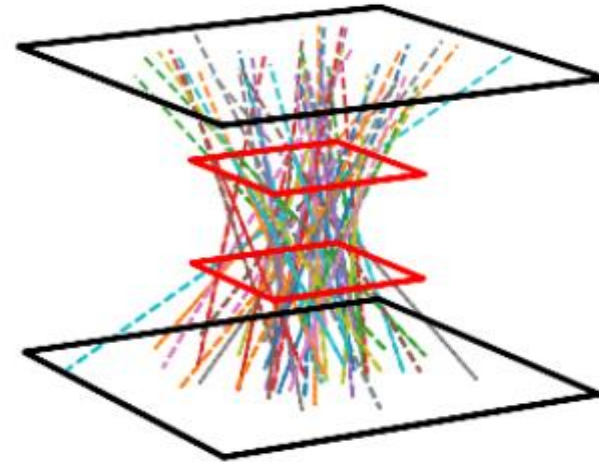
# UNIANDES GEM DETECTORS



# X-ray test with a full readout GEM detector



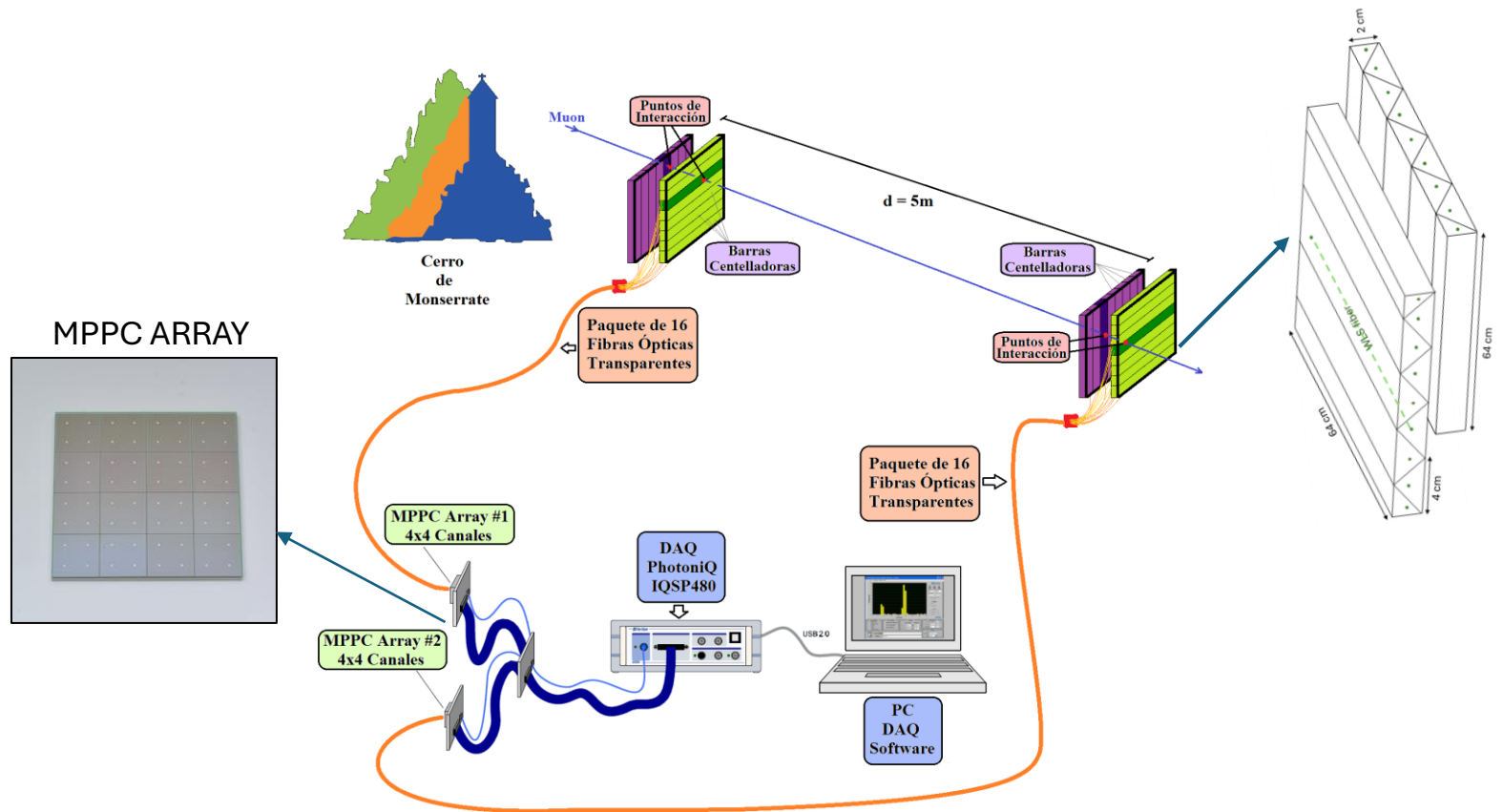
# Atmospheric muon tracking with a full readout GEM detector



- Still need to improve efficiency: ~80% for each GEM detector
- 24/7 operation requires further improvements in daq stability, specially temperature.

# Scintillation matrix readout by SiPMs

## Hodoscope



1. Carlos A. Avila, Luis M Mendoza, Gerardo Alfonso Roque, Leonardo Loaiza, Jorge M. Racedo Roberto J. Rueda, "Feasibility study of a TIMEPIX detector for mammography applications", Proc. of SPIE Vol. 10572 105720Z-2, <https://doi.org/10.1117/12.2285910>
2. Juan Sebastián Calderón García, Gerardo Roque and Carlos Avila, "Construction of mammography Phantoms with a 3D printer and tested with a TIMEPIX system", Proc. of SPIE Vol. 10572 ,105720Y (2017), <https://doi.org/10.1117/12.2285897>
3. J.S. Useche Parra and C. Avila, "Estimation of cosmic-muon flux attenuation by Monserrate Hill in Bogota", *Journal of Instrumentation* 14 P02015, 2019, <https://doi.org/10.1088/1748-0221/14/02/P02015>
4. S. Procz, C. Avila, J. Fey, G. Roque, M. Schuetz, E. Hamann, "X-ray and gamma imaging with Medipix and Timepix detectors in medical research", Radiation Measurement, Vol. 127, 2019, <https://doi.org/10.1016/j.radmeas.2019.04.007>
5. C. Navarrete, S. Procz, M. Schütz, G. Roque, J. Fey, C. Avila, A. Olivo, M. Fiederle, "Spectral X-ray phase contrast imaging with a CdTe photon-counting detector", Nuclear Instruments and Methods in Physics Research Section A, Volume 971, 2020, <https://doi.org/10.1016/j.nima.2020.164098>
6. S. Procz, G. Roque, C. Avila, J. Racedo, R. Rueda, I. Santos, M. Fiederle, "Investigation of CdTe, GaAs, Se and Si as Sensor Materials for Mammography", *IEEE Transactions on Medical Imaging*, June 2020, doi: 10.1109/TMI.2020.3004648, <https://doi.org/10.1109/TMI.2020.3004648>
7. S. Procz, G. Roque, M. Perez, L. Mendoza, C. Avila, "Study of Contrast-to-Noise Ratio performance of a Medipix3RX CdTe Detector for Low Dose Mammography Imaging", Nuclear Instruments and Methods in Physics Research Section A, Volume 992, 2021, <https://doi.org/10.1016/j.nima.2020.165000>
8. C. Avila. G. Roque, J. S. Calderon, Patente, "Fantoma de Calibración y diagnóstico", Octubre 2022, SIC 054-2019
9. C. Borja C. Avila, G. Roque, M. Sanchez, "Atmospheric Muon Flux Measurement near Earth's Equatorial Line ", *Instruments* **2022**, 6(4), 78; <https://doi.org/10.3390/instruments6040078>
10. J. S. Useche Parra, M.K. Schütz G. Roque, J. Fey, C. Avila, M. Fiederle and S. Procz, "Dose estimation in X-ray backscatter imaging with Timepix3 and TLD detectors", *JINST* **18** P05042 <https://dx.doi.org/10.1088/1748-0221/18/05/P05042>
11. J Bermúdez, G Roque, J Calderón, P Pardo, M Sánchez, V Ramos, C Ávila, "3D phantom for image quality assessment of mammography systems", *Phys Med Biol.* 2023 Oct 13; 68(20). <https://doi.org/10.1088/1361-6560/acfc10> PMID:37733054 .
12. L. Mendoza, C. Avila, R. Rodríguez L. Loaiza and G. Roque. "CNR performance of semiconductor materials for X-ray imaging of breast calcifications", *JINST* **18** T11001, ). <https://doi.org/10.1088/1748-0221/18/11/T11001>

= Nombre de estudiante participando del estudio



# GRACIAS!